Bifurcation Analysis of Liesegang Ring Pattern Formation

M. I. Lebedeva,[1] D. G. Vlachos,[1,*] and M. Tsapatsis[2]

[1]*Department of Chemical Engineering and Center for Catalytic Science and Technology, University of Delaware, Newark, Delaware 19716-3110, USA*

[2]*Department of Chemical Engineering, University of Massachusetts–Amherst, Amherst, Massachusetts 01003-3110, USA*

(Received 3 June 2003; published 24 February 2004)

Bifurcation analysis is introduced to a prototype Liesegang ring (LR) model to explain pattern formation as an instability of a propagating plane reaction front. A theoretical criterion for the onset of patterning is derived and numerically tested. The uneven spacing law of LR bands is explained as a consequence of the time varying velocity of the moving reaction front. Suggestions for controlling pattern formation are provided.

DOI: 10.1103/PhysRevLett.92.088301 PACS numbers: 82.40.Ck, 05.45.-a, 47.70.–n, 89.75.Kd

Patterning of materials is desirable for the development of devices with applications ranging from electro-optics and photonics to microreactors and biosensors. Most of the current techniques for materials patterning rely on top-down processing by removing material from predetermined locations. Bottom-up strategies such as self-organization routes are also intensively pursued. Understanding the mechanisms driving self-organization is of high interest and can impact the evolving area of nanotechnology.

One of the best-known mechanisms of materials patterning is based on the Liesegang rings (LR) mechanism [1]. LR patterns or bands typically form when a soluble reactant diffuses either from the center or the periphery of a medium uniformly filled with the second soluble reactant to produce an insoluble substance. In most experiments, bands obey an uneven spacing law when the ratio of the positions of consecutive bands tends to a constant value.

Despite intensive theoretical work devoted to LR formation, e.g., Refs. [2–8], there remain a number of experimental observations that have not been explained. As an example, patterns form only under certain conditions, but the reason is poorly understood. While prenucleation models [2,9] can explain the spacing law, a numerical solution of the complete diffusion-reaction model does not even predict bands (see [10] and references therein). Furthermore, the spatial periodicity of bands of nanocrystalline TiO_2 in mesoporous Vycor [11], which is either nearly constant or obeys the aforementioned spacing law under different conditions, cannot be easily rationalized. Development of theory can be invaluable in understanding the onset of LR pattern formation and in creating strategies for experimental control.

In this Letter, we study LR pattern formation using nonlinear systems theory. In particular, we cast for the first time the LR pattern formation problem as an instability of a spatially inhomogeneous traveling wave solution to derive a theoretical criterion that can clarify the onset of this phenomenon. Numerical simulations are then used to qualitatively verify theoretical predictions. Finally, comparisons to experiments and suggestions for controlling LR pattern formation are made.

An analysis is performed for a prototype LR model consisting of two parallel reactions

$$A + B \xrightarrow{k_1} S \quad \text{and} \quad A + B \xrightarrow{S,k_2} S. \tag{1}$$

The first reaction converts reactants to form a nucleus S, once some critical concentration has been reached. The second reaction depletes the reactants via growth, after a nucleus has formed. Because of its surface area dependence, the second reaction is typically autocatalytic in nature. This is a critical issue regarding LR pattern formation.

The dimensionless governing equations for species A, B, and S are, respectively,

$$\frac{\partial y_1}{\partial t} = \frac{\partial^2 y_1}{\partial x^2} - f(y_1, y_2, z), \tag{2}$$

$$\frac{\partial y_2}{\partial t} = D\frac{\partial^2 y_2}{\partial x^2} - \sigma f(y_1, y_2, z), \tag{3}$$

$$\frac{\partial z}{\partial t} = \sigma f(y_1, y_2, z). \tag{4}$$

The following dimensionless quantities are used: $y_1 = C_A/C_A^0$, $y_2 = C_B/C_B^0$, $z = C_S/C_B^0$, $D = D_B/D_A$, $\sigma = C_A^0/C_B^0$, $t = t'D_A/L^2$, and $x = x'/L$. Here C_i stands for concentration of species i, D_i for diffusivity, and x', x and t', t are the real and dimensionless length and time coordinates, respectively. Initially species B is in uniform concentration, C_B^0, in the entire domain $0 \le x' \le L$, whereas A and S are not present. Zero-flux boundary conditions are applied to both species A and B at $x' = L$, whereas the concentration of A at $x' = 0$, C_A^0 is assumed to be constant. Finally, we assume that nucleation occurs when the product $C_A C_B$ exceeds some critical value K_s, as has often been previously assumed, e.g., in Refs. [5,10]. With these assumptions, the form of the

dimensionless reaction function f is $f = \kappa y_1 y_2 (H(y_1 y_2 - y_c) + \gamma z^{\nu})$, with $\nu > 0$, $\kappa = k_1 C_B^0 L^2 / D_A$, $\gamma = k_2 C_B^0 / k_1$, and $y_c = K_S / C_A^0 C_B^0$. H is the Heaviside step function. The key parameters are the critical supersaturation y_c, the ratio γ of autocatalytic growth and nucleation rate constants, and κ.

Numerous simulations of (2)–(4) show distinct deposition modes. Examples are shown in Fig. 1. In one growth mode, termed frontal propagation [panel (a)], a continuous deposit forms as a result of a concentration wave propagating through the entire substrate. In another growth mode [panel (b)], termed quasiperiodic, bands form from the beginning [near the left boundary of Fig. 1(b)]. Finally, quasiperiodic deposition often starts after some induction time, i.e., a mixed mode of frontal growth at the beginning followed by quasiperiodic growth at longer times has also been observed (see Fig. 3 below for examples of this mode).

Simulations indicate that LR bands appear only when both y_c and γ are nonzero and sufficiently large. The effect of the critical concentration is expected, and it is consistent with Ostwald's nucleation theory [2]. However, it is interesting to note that there appears to be a criticality associated with γ. Our simulations indicate that the frontal growth gives place to quasiperiodic deposition when the autocatalytic reaction is sufficiently faster than the nucleation step. Theoretical analysis is employed to explain these observations.

We start from the frontal growth mode and consider a time interval between some initial moment and the moment when deposition occurs near the end of the domain. In this case the concentration profiles $y_2(x, t)$ (reactant B) and $z(x, t)$ (deposit S) have traveling wavelike features; i.e., as time increases the profiles translate along the x coordinate [Fig. 1(a)]. Unlike real traveling wave solutions, these waves move with nonconstant, slowly varying velocity $\omega(t)$. It is well-known that $\omega \sim \lambda/\sqrt{t}$, where λ is some nonlinear function of initial concentrations C_A^0, C_B^0 and diffusion coefficients D_A and D_B (e.g., [4,12]). Nevertheless, simulations show that each of these waves with instant velocity $\omega(t)$ is asymptotically close (except

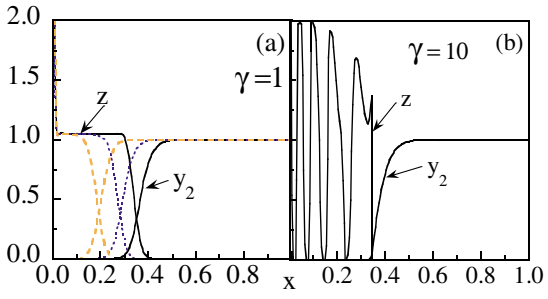

FIG. 1 (color online). Deposit and species B concentration after some time depicting (a) frontal deposition ($\gamma = 1$) at times $t = 0.035$, 0.055, and 0.075 (from left to right) and (b) quasiperiodic deposition ($\gamma = 10$). The other parameters are $\sigma = 5$, $\kappa = 370.4$, $\nu = 1$, $D = 0.11$, and $y_c = 0.15$.

for translation) to the real traveling wave solution $y_2 = Y_2(x - \omega(t)\tau)$, $z = Z(x - \omega(t)\tau)$ of

$$\frac{\partial y_2}{\partial \tau} = D\frac{\partial^2 y_2}{\partial x^2} - \sigma F(y_2, z, t), \qquad \frac{\partial z}{\partial \tau} = \sigma F(y_2, z, t), \tag{5}$$

where t is a parameter, and $\omega(t)$ is the constant front velocity for this solution corresponding to fixed parameter t. Equation (5) is subject to boundary conditions $y_2 = y^-$, $z = z^-$ at $x \to -\infty$; $y_2 = 1$, $z = 0$ at $x \to \infty$ where $0 \le y^- < 1$ and $z^- > 0$ are constant. The function $F(y_2, z, t) = f[y_1(y_2(x, t)), y_2(x, t), z(x, t)]$ is determined by the solution of (2)–(4) at this fixed t; i.e., since $y_2(x, t)$ is monotonic, we regard x as a function of y_2 and rewrite function $y_1(x, t)$ in terms of the independent variable y_2, namely, $y_1(x, t) = y_1(y_2, t)$. We can construct such a function numerically for each fixed value t. So (5) is obtained for y_2 and z only and can be solved starting from initial functions $y_2^0 = y_2(x, t)$ and $z^0 = z(x, t)$ which are the solution of (2)–(4) at the same t. Now τ is the time variable. Simulations reveal that the solution of (5) is the same pair of functions $y_2(x, t)$, $z(x, t)$, which move along the x axes with velocity $\omega(t)$ as τ increases. Thus, the solutions of (2)–(4), $y_2(x, t)$ and $z(x, t)$ [not $y_1(x, t)$], may be seen as quasistationary states (QSS) in the transition from an initial to a final state.

The resulting growth mode depends on the character of these intermediate states. A similar phenomenon is known for the time evolution of autocatalytic processes [13]. In particular, for the cubic autocatalysis with catalyst decay, the concentrations of reactants tend to an oscillatory motion around their quasistationary values when the latter become unstable. Unlike the autocatalyis problem, here the stability of traveling waves needs to be analyzed. The frontal growth mode exists as long as the traveling waves are stable. Our aim is to find a criterion for their stability.

Figures 2(a) and 2(b) show the front position and velocity, respectively, vs time for the cases depicted in Fig. 1. Under some conditions ($\gamma = 1$), a wave with almost constant speed propagates through the substrate. Increase of the autocatalytic reaction rate ($\gamma = 10$) leads to instability of the QSS and to quasiperiodic growth mode.

We employ the QSS hypothesis to analyze the growth modes and the transition from frontal propagation to quasiperiodic deposition. This hypothesis holds in the case of strong concentration gradients. Also the function F must satisfy some conditions in order for the asymptotic correlations $y_2(0, t) \approx y^-$, $z(0, t) \approx z^-$ and $y_2(1, t) \approx 1$, $z(1, t) \approx 0$ to hold at the ends of the domain $0 \le x \le 1$. Simulations indicate that they hold when the kinetic rate constants are large enough. Thus below we theoretically focus on the case where $\kappa \gg 1$.

We examine first the case where the autocatalytic step in (1) is absent ($\gamma = 0$) and the critical supersaturation is $y_c \ge 0$. We consider Eqs. (2) and (3) only and the

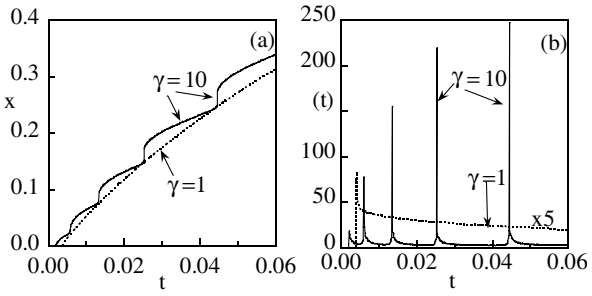

FIG. 2. Front position (a) and front velocity (b) for the two deposition modes of Fig. 1.

quasistationary solution is the traveling wave solution of the first of Eqs. (5). It is known [14] that this solution exists, is unique (except for translation), and is stable if the function $F(y_2, t)$ satisfies some conditions. It follows from the analysis of Eqs. (2) and (3) that these conditions hold for the function F. For $y_c = 0$, the left boundary condition is $y^- = 0$, $z^- = 1$; for $y_c > 0$, it is $y^- > 0$, $z^- = 1 - y^-$, where $y_2 = y^-$ is determined from the equation $y_1(y_2)y_2 = y_c$. Thus in the absence of the autocatalytic reaction ($\gamma = 0$), frontal deposition takes place even when a critical supersaturation exists $y_c > 0$. Our analysis demonstrates that Ostwald's assumption [2] of discontinuous nucleation is necessary (but not sufficient) for LR pattern formation and explains the apparent paradox discussed in [10], i.e., why the full diffusion-reaction model cannot predict bands.

Next we consider the case where both autocatalysis and nucleation occur, i.e., $y_c > 0$ and $\gamma > 0$. It is interesting to note an analogy between this behavior and the combustion of condensed systems. Experiments show that the velocity of flame propagation exhibits periodic pulsation for some conditions. Furthermore, the burned samples have a layered structure normal to the flame front. Formally the model of these processes has the form of Eqs. (5) and was analyzed in detail in [15] using the narrow reaction zone approximation. It was assumed that the chemical reaction occurs at the front, say at $\xi = 0$, where $\xi = x + \Omega(\tau, t)$ is the moving coordinate system and $x = -\Omega(\tau)$ is the coordinate of the nonsteady moving reaction front. The function $\sigma F(y_2, z, t)$ is approximated as $\sigma F(y_2, z, t) \sim \psi(y_2, t)\delta(\xi)$, where $\delta(\xi)$ denotes the Dirac delta function. Linear stability analysis of Eqs. (5) shows [15] that its solution is unstable for $\phi > \phi_c = 2 + \sqrt{5}$, where $\phi = -\psi'_{y_2}(y_2^0(0), t)/\omega(t)$, and $y_2^0(\xi)$ is the steady solution of (5) in the narrow reaction zone approximation [$\Omega(\tau, t) = -\omega(t)\tau$ for a steadily propagating reaction front, $y_2^0 = 1 - e^{-\omega\xi/D}$ for $\xi > 0$, and $y_2^0 = 0$ for $\xi < 0$]. The analysis in [15] shows that a Hopf bifurcation occurs, giving rise to a stable time periodic traveling wave solution that leads to a spatial pattern in the x domain.

In our case the function F is not an explicit function of y_2 but is the result of the solution of the model (2)–(4). However, we can still analyze the effect of parameters on the stability of the traveling wave solution of Eqs. (5). We apply the result of [15]. To obtain an expression for the source strength ψ, we employ an asymptotic analysis with respect to $\kappa^{-1} \ll 1$. The method of analysis is similar to that used in [16]. The function F can be written as $F(y_2, z, t) = F_1 + F_2$, where $F_1 = \kappa y_1(y_2)y_2 H$ and $F_2 = \kappa\gamma y_1(y_2)y_2 z$ ($\nu = 1$). In our specific system, the narrow reaction zone implies that in front of the reaction front ($\xi > 0$) nucleation happens and $F = F_1$, whereas behind the front ($\xi < 0$) only autocatalytic growth occurs; i.e., $F = F_2$.

We consider Eqs. (5) in a moving coordinate system and introduce a stretched coordinate ($\chi = \kappa\xi$) inside the reaction zone. Furthermore, we introduce the outer and the inner expansions of the functions $y_2(\xi, \tau)$, $z(\xi, \tau)$ and $\omega(t)$, $\Omega(\tau, t)$ with respect to the small parameter κ^{-1}. Substituting the inner expansions into Eqs. (5), expanding the nonlinear terms F_1 and F_2 in powers of κ^{-1}, and matching with the outer solutions, we obtain for the lowest order approximation $\psi(y_2(0, \tau), t) = \{2\sigma D y_c \kappa[\gamma(y^-(t) - y_2(0, \tau)) + \Delta y(t)]\}^{1/2}$ and $\psi(0, t) = \{2\sigma D y_c \kappa(\gamma y^-(t) + \Delta y(t))\}^{1/2} = \omega(t)$, where $\Delta y = y^+ - y^-$, with y^+, y^- ($y^+ > y^-$) being the solutions of the equation $y_1(y_2)y_2 = y_c$. Then the result of [15] implies that instability happens when a parameter ϕ becomes

$$\phi = \sigma D\gamma y_c \kappa/\omega^2(t) = K_S k_2 D_B t'/\lambda^2 D_A > 2 + \sqrt{5}. \quad (6)$$

The second equality is obtained for the case when the first reaction in (1) is considered fast. Then the dimensional front velocity, $u(t') = \omega(t)D_A/L$, is $u(t') = \lambda\sqrt{D_A/t'}$ [4]. Equation (6) shows explicit dependence on t'. It is the main theoretical result of our analysis. Fast autocatalytic kinetics and large values of critical supersaturation are prerequisites for band formation for large κ and strong concentration gradients.

Equation (6) is consistent with simulation results shown in Fig. 3 for various combinations of parameters. These simulations confirm that when the dimensionless parameters appearing in the numerator of Eq. (6) are small (large), frontal propagation (quasiperiodic deposition) occurs. The speed of the traveling wave [denominator of Eq. (6)] is also essential in determining whether instability occurs or not and explains the mixed growth mode. Specifically, one can see from (2)–(4) and the corresponding boundary conditions that, as time t increases, the quasistationary velocity $\omega(t)$ decreases due to the diffusion time needed for A to reach the reaction front [see also Fig. 2(b)]. Thus, there exists a time t^* when the value of $\omega(t^*)$ becomes small enough, so that (6) is satisfied. Then the traveling wave becomes unstable. The change of the speed of the traveling wave with time explains then the presence of an induction time or length of an initial "plug" zone, $x_p \sim \omega(t^*)t^*$, giving rise to the appearance of the mixed growth mode depicted in Fig. 3 for some parameters. Thus when the domain is thin enough the growth mode may be frontal. The simulations

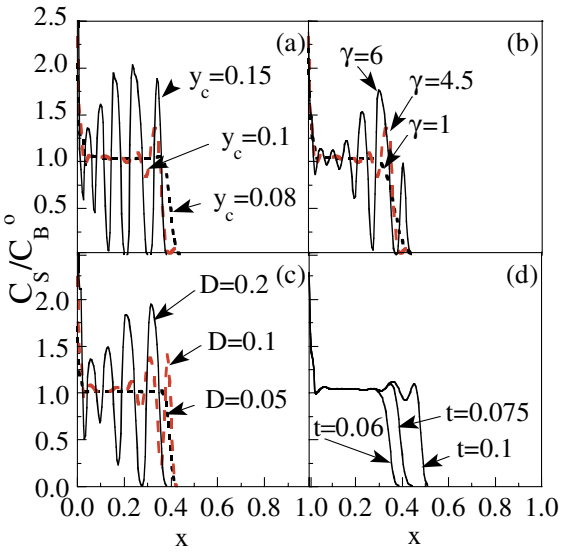

FIG. 3 (color online). Panels (a)–(c) show examples for verifying (6): (a) effect of critical supersaturation, (b) effect of the rate constant of the autocatalytic step, and (c) effect of diffusivity of reactant B. All curves in (a)–(c) correspond to the same time, $t = 0.07$. Panel (d) shows the decrease of the plane front velocity ω with time: at $t = 0.06$: $\omega = 4.4$, $\phi = 4.24$; at $t = 0.075$: $\omega = 3.8$, $\phi = 4.9$; at $t = 0.1$: ω oscillates with t. The parameters are $\sigma = 5$, $\kappa = 370.4$, $\nu = 1$ with (a) $\gamma = 4.5$, $D = 0.11$, (b) $y_c = 0.1$, $D = 0.11$, (c) $\gamma_c = 5$, $y_c = 0.1$, and (d) $\gamma = 3.5$, $y_c = 0.1$, $D = 0.11$.

of Fig. 3(d) show that the transition to quasiperiodicity happens for parameters satisfying nearly quantitatively (6) (see the caption for details). Therefore, by controlling the temperature and the initial concentrations, it could be possible to alter the wave speed and thus the position where patterns start to form and possibly the wavelength of the patterns. An important point is that our theory provides a means of computing the plug distance from an estimation of the wave speed either experimentally or from simulations under frontal propagation conditions.

The presence of criticality depicted by (6) rationalizes why simulations for prenucleation models proposed in [2,5] cannot produce LR bands (see [10]). Furthermore, the form of the function f and its parameters are also important in determining whether patterns form or not.

Next we draw analogies to condensed combustion systems. Combustion experiments and associated models exhibit self-sustained oscillations, whereas deposition obeys usually uneven spacing and time laws. The reason is that the source function $F(y_2, z, t)$ and the instant quasistationary front velocity $\omega(t)$ are functions of time, giving rise to qualitatively different behavior. It is expected that, for a relatively time independent source F, regular periodic patterns would develop. This may be achieved experimentally in different ways. For example, simulations by introducing "convective" terms into the governing equations lead to more regular deposition patterns (not shown). This implies that deposition in materials of larger pores will be affected by convection and may give more regular patterns. A similar effect was described in [4] where an electrical field was applied to an interdiffusion precipitation system. Also simulations performed for a hypothetical reaction-diffusion model [17] show formation of equidistant bands due to an autocatalytic chemical front of constant velocity.

Finally, we note that helical deposition structure was described in [6]. It was shown that there exists a solution corresponding to a spiral when the radius of the test tube is large enough. Based on the criticality demonstrated here, it may be possible to also explain the appearance of such growth modes as a bifurcation from a plane reaction front, when the test tube radius exceeds a critical value. Future work is needed to explore this issue.

In summary, we have derived for the first time a theoretical criterion for the appearance of LR patterns using nonlinear systems theory and subsequently tested via numerical simulation. Our theoretical analysis is capable of explaining different deposition modes including frontal propagation, quasiperiodic, and mixed mode. The periodicity of LR patterns is a function of the velocity of a traveling wave, suggesting that well designed experiments could be used to control LR formation. Our findings can guide experiments in pattern formation driven by diffusion-reaction instability.

*Corresponding author.

[1] R. E. Liesegang, Naturwiss. Wochenschr. **11**, 353 (1896).
[2] W. Ostwald, *Lehrbuch der allgemeinen Chemie* (Engelmann, Leipzig, 1897).
[3] D. Feinn, P. Ortoleva, W. Scalf, S. Schmidt, and M. Wolff, J. Chem. Phys. **69**, 27 (1978).
[4] R. Feeney, S. L. Schmidt, P. Strickholm, J. Chadam, and P. Ortoleva, J. Chem. Phys. **78**, 1293 (1983).
[5] S. Prager, J. Chem. Phys. **25**, 279 (1956).
[6] D. S. Chernavskii, A. A. Polezhaev, and S. C. Muller, Physica D (Amsterdam) **54**, 160 (1991).
[7] T. Antal, M. Droz, J. Magnin, and Z. Racz, Phys. Rev. Lett. **83**, 2880 (1999).
[8] G. T. Lee, Phys. Rev. Lett. **57**, 275 (1986).
[9] G. Venzl, J. Chem. Phys. **85**, 2006 (1986).
[10] H. K. Henisch, *Crystals in Gels and Liesegang Rings* (Cambridge University Press, Cambridge, 1988).
[11] M. Tsapatsis, D. G. Vlachos, S. J. Kim, H. Ramanan, and G. R. Gavalas, J. Am. Chem. Soc. **122**, 12864 (2000).
[12] L. Galfi and Z. Racz, Phys. Rev. A **38**, 3151 (1988).
[13] P. Gray and S. K. Scott, *Chemical Oscillations and Instabilities, Nonlinear Chemical Kinetics* (Clarendon Press, Oxford, 1990).
[14] A. I. Volpert and V. A. Volpert, Nonlinear Anal. Theory Methods Appl. **49**, 113 (2002).
[15] B. J. Matkowsky and G. J. Sivashinsky, SIAM J Appl. Math. **35**, 465 (1978).
[16] S. B. Margolis, SIAM J Appl. Math. **43**, 351 (1983).
[17] I. Lagzi and D. Karman, Chem. Phys. Lett. **372**, 831 (2003).